VISIBLE LIGHT-ACTIVATABLE CYCLODEXTRIN-CONJUGATES FOR THE EFFICIENT DELIVERY OF NITRIC OXIDE WITH FLUORESCENT REPORTER AND THEIR INCLUSION COMPLEXES WITH BETAXOLOL

Mimimorena Seggio,[a] Sara Payamifar,‡[ab] Aurore Fraix,[a] Eszter Kalydi,[cd] Petr Kasal,[e] Ovidio Catanzano, [f] Claudia Conte, [g] Fabiana Quaglia [*g] and Salvatore Sortino [*a]

a PhotoChemLab, Department of Drug and Health Sciences, University of Catania, Catania, Italy. E-mail: ssortino@unict.it

b Organic Chemistry Institute for Advanced Studies in Basic Sciences (IASBS), Zanjan, Iran

c CycloLab Ltd., Illatos u´t 7, H-1097 Budapest, Hungary d Department of Pharmacognosy, Semmelweis University, H-1085 U¨ ll+oi u´t 26, Budapest, Hungary

e Department of Organic Chemistry, Charles University in Prague, Hlavova 8/8 128 43, Prague 2, Czech Republic

f Institute for Polymers, Composites and Biomaterials, CNR, Via Campi Flegrei 34, 80078 Pozzuoli, Napoli, Italy

g Drug Delivery Laboratory, Department of Pharmacy, University of Napoli Federico II, Via Domenico Montesano 49, 80131, Napoli, Italy. E-mail: quaglia@unict.it †

Electronic supplementary information (ESI) available. See DOI: 10.1039/ d1nj00039j

‡ S. P. carried out the work at the University of Catania during her stage from the IASBS.

Abstract

This contribution reports the design, synthesis, photochemical properties and drug inclusion capability of two novel b-cyclodextrin (bCD) conjugates, bCD-NBFNO1 and bCD-NBFNO2, covalently integrating an N-nitroso amino-nitro-benzofurazan in the primary and secondary hydroxyl rims of the bCD scaffold, respectively through flexible spacers of different length. Both bCD conjugates are water-soluble and release nitric oxide (NO) under the input of either blue or green light, with quantum yields F_{NO}(blue) = 0.13, 0.31 and F_{NO}(green) = 0.007, 0.013 respectively, the former representing the largest values ever reported for nonmetal-containing NO donors activatable by visible light. The good contrast between the

fluorescence green emission of the chromogenic moiety after and before the NO release permits the easy and in realtime quantification of the amount of NO generated, without the addition of external fluorescent agents. Despite the presence of the appendages, these bCD derivatives are also able to complex betaxolol, a b-blocker drug widely used for the reduction of the intraocular pressure, with binding constants K_b = 500 50 and 1100 100 M_1, respectively, without affecting the photochemical performances. In view of the wellknown vasodilator properties of NO, the present bCD derivatives represent intriguing candidates for biopharmaceutical research studies addressed to combined therapeutic ocular applications

1. Introduction

The design of molecules able to generate nitric oxide (NO) has received increasing attention, especially over the last decade.[1,2] This is due to the multifaceted role NO plays in a number of physiological processes including neurotransmission, vasodilatation and hormone secretion,[3] and its superb antioxidant, anticancer and antibacterial activity.[4] NO has shown vasodilator effects on eye vasculature[5–7] and wound healing effect on injured corneal surface opening new therapeutic perspectives in ophthalmology.[8–10] This scenario has given a boost to the development of compounds able to release NO under physiological conditions as potential therapeuticals to fight a variety of diseases.[1,2,11,12] The strict dependence of the biological effects of NO by its dosage and location[13] has made NO-photodonors (NOPD) more appealing than spontaneous NO releasers due to the superb spatiotemporal accuracy that light triggering offers.[14–18] In particular, NOPD activation by environmental light can be very suited for supplying NO for therapeutic purposes.[19,20] Unfortunately, most NOPD have poor water solubility requiring specific formulations for their delivery to the anterior segment of the eye. Among the strategies available to tackle this issue, the use of cyclodextrins (CDs) used for decades to increase the watersolubility of lipophilic drugs still offers room to innovate. CDs are cyclic oligosaccharides, well-known for their capability to complex, stabilize and solubilize guest compounds.[21–25] CD solubilizing activity is strictly related to their aptitude to form supramolecular complexes with a guest molecule while covalent modification of the CDs ring through functionalization of the primary and/or secondary hydroxyl groups with suitable appendages has been much less explored. The integration of photoresponsive units into the CDs scaffold is of great interest as recently proven by a variety of photoresponsive CD-based nanoconstructs with potential phototherapeutic applications.[26,27] Several NOPD have been supramolecularly combined with CDs

derivatives.[28] In contrast, only limited examples of NO photodonor covalent conjugates with CDs are reported to date.[29,30] In the context of ocular diseases, the covalent modification of the CD with NOPD could bring the benefit of obtaining a functional NO-releasing scaffold whilst, at the same time, maintaining the macrocycle capacity for encapsulation of small therapeutics in a combinatory therapeutic approach.[29–32] In this contribution, we provide a proof of concept of this approach by synthesising two novel bCD conjugates, bCD-NBFNO1 and bCD-NBFNO2, integrating an N-nitroso amino-nitro-benzofurazan (NBF-NO) within the primary and secondary rim of the bCD scaffold, respectively through flexible spacers of different length (Scheme 1). The N-nitroso amino-nitro-benzofurazan photoresponsive unit was selected since it represents the non-metal based NO releaser generating NO with the highest quantum yield upon excitation with Vis light developed so far.[33] Concomitantly to NO release, this compound forms the highly fluorescent non-nitrosated derivative as the sole stable photoproduct, representing an optical reporter useful for the NO detection even at the naked eye. Despite the excellent photochemical performances, NBF-NO has poor solubility in an aqueous medium, which severely limits its ocular application in the absence of any carrier system. After an in depth characterization of the photophysical properties of the bCD conjugates, we explore their host–guest complexation properties with betaxolol (BTX), a well-known b-blocker drug used against glaucoma for the reduction of intraocular pressure.[34,35]

2. Experimental

2.1. Materials

All reagents (Sigma-Aldrich, Alfa Aesar, Molar Chemicals Kft and Cyclolab) were of high commercial grade and were used without further purification. All solvents used (from Carlo Erba) were spectrophotometric grade. Synthetic procedures All bCD conjugates were synthesized according to the procedures reported in ESI.

2.2. Instrumentation

$_1$H-NMR spectra were recorded on a Varian VXR-600 at 600 MHz. UV-Vis spectra absorption and fluorescence emission spectra were recorded with a JascoV-560 spectrophotometer and a Spex Fluorolog-2 (mod. F-111) spectrofluorimeter, respectively, in air-equilibrated solutions, using quartz cells with a path length of 1 cm. Fluorescence lifetimes were recorded with the above fluorimeter equipped with a TCSPC Triple Illuminator.

The samples were excited with a pulsed diode excitation source (Nanoled) at 455 nm, the decays were monitored at 550 nm, and ethanol solution itself was used to register the prompt at 455 nm. The system allowed a time-resulution4200 ps. The multiexponential fit of the fluorescence decay was obtained by the following equation: $I(t) = Sa_i\exp(_{t/ti})$ Absorption spectral changes were monitored by irradiating the sample in a thermostated quartz cell (1 cm path length, 3 mL capacity) under gentle stirring, using a continuum laser with I_{exc} = 405 nm, 20 mW, and I_{exc} = 532 nm, ca. 100 mW, and having a beam diameter of ca. 1.5 mm. Direct monitoring of NO release in solution was performed by amperometric detection (World Precision Instruments), with an ISO-NO meter, equipped with a data acquisition system, and based on direct amperometric detection of NO with short response time (o5 s) and sensitivity range 1 nM–20 mM. The analogue signal was digitalized with a four-channel recording system and transferred to a PC. The sensor was accurately calibrated by mixing standard solutions of $NaNO_2$ with 0.1 M H_2SO_4 and 0.1 M KI according to the reaction: $4H_+ + 2I + 2NO_2 - 2H_2O + 2NO + I_2$ Irradiation was performed in a thermostated quartz cell (1 cm path length, 3 mL capacity) using the continuum laser with I_{exc} = 405 nm or 532 nm. NO measurements were carried out under stirring with the electrode positioned outside the light path in order to avoid NO signal artefacts due to photoelectric interference on the ISO-NO electrode.

2.3. Fluorescence and photodecomposition quantum yields

Fluorescence quantum yields (F_f) were determined using optically-matched solutions at the excitation wavelength of conjugates and Fluorescein NaOH 0.1 M as reference (F_{ref} = 0.95)[36] through the following equation: $F_f = F_{f(s)}(I/I_{(s)})$ where $F_{f(s)}$ is the fluorescence quantum yield of the standard; I and $I_{(s)}$ are the areas of the fluorescence spectra of compounds and standard, respectively; absorbance at the excitation wavelength was less than 0.1 in all cases. Photodecomposition quantum yield (F_{NO}) was determined at I_{exc} = 405 nm and 532 nm within the 20% transformation of the conjugates by using the following equation $F_{NO} = [C]V/t(1–10_A)I$ where [C] is the concentration of phototransformed bCDNBFNO1 or bCD-NBFNO2, V is the volume of the irradiated sample, t is the irradiation time, A is the absorbance of the sample at the excitation wavelength and I the intensity of the excitation light. The concentration of the phototransformed conjugates was determined spectrophotometrically, by taking into account the absorption changes at 385 nm and the related De at the same wavelength. I was calculated by potassium ferrioxalate actinometry.

2.4. Dark stability tests

The stability of both conjugates in the dark was evaluated by recording the absorption spectra of water solution of each compound in thermostated baths at different temperatures. The percent of decomposition was evaluated by the changing of the absorption spectra, taking into account the molar extinction coefficients of the starting compounds and their respective non-nitrosate derivatives.

2.5. Host–guest complexation experiments with BTX

To 2 ml of an aqueous solution of BTX (1.4 x 10^{-3} M), different volumes of either bCD-NBFNO1 or bCD-NBFNO2 stock solutions (6 x 10^{-3} M) were added. After the addition of each aliquot, the solutions were stirred for 5 min, and the absorption spectra were recorded. The spectral changes were evaluated by subtracting the absorption of the same concentration of conjugates in neat water. The absorbance changes were then plotted as a function of the concentration of the conjugates according to the Benesi–Hildebrand equation (vide infra).

3. Results and discussion

bCD-NBFNO1 and bCD-NBFNO2 show excellent solubility in water up to ca. 10 2 M. Fig. 1 shows the UV-Vis spectroscopic properties of aqueous solutions of the two derivatives and, for the sake of comparison, those of the non-nitrosated bCD conjugates bCD-NBF1 and bCD-NBF2. The absorption spectra of bCD-NBFNO1 and bCD-NBFNO2 (Fig. 1A) exhibit a dominant absorption at ca. 380 nm and a shoulder at 475 nm. The main absorption is blue-shifted by more than 90 nm as compared to that of the non-nitrosated analogues (see Fig. 1B) as a consequence of the loss of the ‘‘charge transfer’’ character due to the presence of the electronwithdrawing NO group at the amino functionality. Note that the shoulder in the visible region is much more intense if compared with that observed for the same chromogenic unit nonlinked to the bCD scaffold.[33] In principle one may think that such absorption can be due to the presence of impurities of non-nitrosate derivative. However, chromatographic analysis (see ESI†) and the photolysis carried out upon irradiation of this band with green light (vide infra) ruled out this hypothesis. In contrast, such a shoulder can be due to either intra or intermolecular non-covalent interaction between the N-nitroso appendages and the bCD moiety. The presence of this absorption, even in very dilute solutions, make the former hypothesis the more likely.[37] Analogously to what already observed for NBF-NO, the presence of the nitroso group has a significant effect on the emission properties. bCD-NBFNO1 and bCD-NBFNO2 exhibited fluorescence emission in

the green region (Fig. 1A) but with quite low quantum yields, being F_f = 0.026 and 0.018, respectively, that are values ca. 4 and 7-fold smaller than those of the analogues non-nitrosated derivatives (F_f = 0. 10 and 0.13) (Fig. 1B). The broad absorption band and the quite large extinction coefficient of the conjugates make possible their excitation in the visible region, even in a reduced concentration range. Fig. 2A shows the absorption and fluorescence emission spectral changes observed upon blue light excitation of an air-equilibrated solution of bCD-NBFNO1. They show the bleaching of the main absorption at 377 nm and the formation of a new, intense absorption band at 475 nm. The spectral evolution is also characterized by the presence of 3 isosbestic points, accounting for a quite clean photochemical process. Note that, the spectrum observed at the end of the photolytic process is identical to that of the non-nitrosated conjugate bCD-NBF1 (compare spectra a in Fig. 1A and B) showing the typical charge transfer band at 475 nm of the amino-nitro-benzofurazan chromogenic unit.[38] Besides, the evolution of the fluorescence emission spectra observed upon irradiation shows a significant restoring of the green emission with I_{max} = 550 nm, typical of the amino-nitrobenzofurazan fluorophore (Fig. 2A).[38] These findings clearly account for the NO photorelease from bCD-NBFNO1 and the concomitant formation of the non-nitrosated fluorophore that act as suitable fluorescent reporter to follow the NO uncaging in real time. The inset of Fig. 2A shows a very good agreement between the evolution of the absorption and fluorescence changes as a function of the irradiation time and indicates that the photolysis was complete within ca. 2 min of irradiation. This accounts for a very effective photochemical reaction as confirmed by the high of the quantum yield for the NO photorelease, F_{NO} = 0.13, a value very close to that observed for the non-water-soluble NBF-NO (F_{NO} = 0.15).[33] NO release was demonstrated by the direct detection of this radical species using an ultrasensitive NO electrode. Fig. 2B shows that NO is promptly released upon illuminator, of the aqueous solution of bCD-NBFNO1, stops in the dark and restarts once the light source is switched on again. Fig. 3A and related inset show that bCD-NBFNO2 exhibited a similar photobehavior with an even higher quantum yield for the NO photorelease, F_{NO} = 0.31, which represents the largest value among those reported for any organic NOPD activatable in the Vis range. Interestingly, the restoring of the emission of the optical reporter is visible even at naked eye (Fig. 3A) and gives easily readable information about the NO generated. The NO photorelease measured by amperometric monitoring was then related to the increase of the fluorescence emission for both compounds. As shown in Fig. 3B, we found a very good correlation between the concentration of NO liberated by both compounds upon light stimuli and the increase of the fluorescence intensity of the related

optical reporters. It needs to be stressed that the remarkable values of F_{NO} found for both conjugates permit the generation of a considerable amount of NO without the need of long irradiation times, which in some cases can be deleterious to cells. According to the literature, anilinyl radical derivatives formed after the homolytic N–NO photocleavage evolves to stable photoproducts by H-transfer from the solvent medium. Since in neat water, like in our case, this process is thermodynamically not feasible, the high values observed for F_{NO} indicate a key role of the bCD scaffold as a reactant, providing a source of 14 easily abstractable H atoms and very close to the anilinyl radical intermediate. Moreover, it should be noted that the absorption and emission spectral and time evolution observed upon irradiation were identical in the case of an N_2-saturated solution (data not shown), suggesting that both the efficiency and nature of the photochemical reaction are not dependent by the presence of oxygen. This observation rules out the participation of a longlived excited triplet state in the photodecomposition, suggesting a NO photodetachment occurring more likely from the short-lived excited singlet state. This hypothesis is supported well by (i) the negligible population of the excited triplet state reported for amino-nitro benzofurazan derivatives in polar solvents,[39] and (ii) the very short singlet lifetimes found for bCD-NBFNO1 and bCD-NBFNO2. As shown in Fig. 4, both conjugates exhibited a biexponential behavior with dominant components (ca. 80%) with t = 2.30 and 0.84 ns, respectively. As discussed above, the absorption spectrum of both bCD conjugates shows a pronounced shoulder extending up to the green region, which is negligible in the case of NBF-NO.[33] These spectral features prompted us to investigate the photoreactivity of the compounds upon excitation with green light. Therefore, aqueous solution of either bCD-NBFNO1 or bCD-NBFNO2 were irradiated at l_{exc} = 532 nm. We observed changes in the absorption and fluorescence emission spectral profiles basically identical to those already observed under blue light stimuli (data not shown) although with lower photochemical efficiency. In fact, the values calculated for F_{NO} were = 0.007 and 0.013 for bCD-NBFNO1 and bCD-NBFNO2, respectively. Fig. 5 shows unambiguous evidence that NO release for both compounds can also be triggered by green light. The photoreactivity dependence by the excitation wavelength is not surprising and may be due to the participation of upper excited singlet states populated with blue light as mediators of the photodecomposition route. The stability of the conjugates was also evaluated in the dark at different temperatures and times. Fig. 6A shows moderate decomposition for both compounds (ca. 20%) at 25 1C, which is almost totally inhibited if samples are incubated for the same time at 4 1C. Moreover, incubation of the solution in a thermostated bath at a different temperature for 15 min each showed

satisfactory stability up to 40 1C (Fig. 6B). Finally, we investigated the host–guest complexation ability of the bCD conjugates. As a prototype guest, we chose BTX for the reasons motivated in the introductory part. Titration of an aqueous solution of BTX was then carried out using increasing amounts of either bCD-NBFNO1 or bCD-NBFNO2. BTX offers good spectroscopic requisite to follow the titration by UV-Vis absorption spectroscopy since its absorption maximum falls at 275 nm, a region in which both conjugates display small absorption. Fig. 7A and B show the absorption spectral changes in the BTX region observed upon the addition of the host molecules and after subtracting the same amount of hosts added to the same volume of water. We observed a hypochromic shift of the absorption band of BTX after addition of the bCD conjugates, according to typical host–guest encapsulation processes. The reciprocal of the absorbance changes at the absorption maximum was then plotted as a function of the reciprocal concentration of the host molecules, according to the Benesi–Hildebrand equation:[40] 1 DA . 1 K_{ass} De .host . 1 De where K_{ass} represents the association constants for the supramolecular host–guest process, De is the difference of the molar extinction coefficient between the free and complexed guest and [host] is the concentration of the bCD conjugates. As shown in Fig. 7C and D, we obtained very good linear plots in both cases and values of K_{ass} of 500 50 M^{-1} and 1100 100 M^{-1} for bCD-NBFNO1 and bCD-NBFNO2, respectively, were obtained from the intercept/slope ratio. The higher value observed for bCD-NBFNO2 is probably attributable to the longer flexible spacer between the CD scaffold and the chromogenic unit, which allows a better accommodation of the host within the hydrophobic cavity. In order to be used in combination, one of the indispensable requisites for this host–guest system is that the encapsulation of BTX in the CD cavity does not affect the photochemical performances of the photoactivatable conjugates. Therefore, photolysis experiments on bCD-NBFNO1 and bCD-NBFNO2 were carried out in the presence of BTX. We observed that the presence of the guest molecule changes neither the nature nor the efficiency of the photoreactivity of both compounds, ruling out any intermolecular communication between the host and the guest through competitive photoinduced processes. This is not a trivial result for host–guest supramolecular complexes. In fact, it is known that the photoreactivity of the host and guest components can be remarkably influenced in efficiency nature or both upon complexation as result of their close proximity and the presence of specific interactions, steric constrains and reduced polarity.[27]

4. Conclusions

We have designed, synthesized and characterized two novel photoactivatable bCD conjugates. These compounds show excellent water solubility, fairly good stability in the dark within 24 h at room temperature, and release of the biologically relevant NO under visible light stimuli. In particular, excitation with blue light leads to NO release with the highest quantum yield never observed for non-metal based NO photoreleaser triggered by visible light. However, although with lower efficiency, both conjugates release NO even under stimuli of green light. The good fluorescence contrast between the highly fluorescent stable photoproducts and the poorly fluorescent starting compounds permits the formers to be excellent optical reporters for the easy detection of the NO generated, with the release process being followed even by the naked eye. Moreover, the reporter can be excited by using the same excitation wavelength used for NO uncaging, facilitating the real-time monitoring of NO, which is crucial given the transient nature of this diatomic radical, without requiring a double excitation source. It is also important to stress that, as extensively demonstrated in our recent studies on other nitroso-derivatives,[41] these photoactivatable compounds do not show significant cytotoxicity in the dark in the concentration range used. Interestingly, functionalization of the CD scaffold with the photoactivatable moieties does not preclude the encapsulation guest as demonstrated by the association of both conjugates with the b-blocker BTX. In this regard, in view of the well-known vasodilator properties of NO, the present work may open intriguing prospects for biological studies on formulations for ocular application against glaucoma, addressed to explore the combinatory effect of BTX and NO, with this latter slowly released at physiological temperature but rapidly released upon environmental light. These studies are currently underway in our laboratories.

Conflicts of interest

We have no confict of interests to declare.

Acknowledgements

We thank the Programma Operativo Nazionale Ricerca e Innovazione 2014–2020 (CCI 2014IT16M2OP005), Fondo Sociale Europeo, Azione I.1 ‘‘Dottorati Innovativi con caratterizzazione Industriale’’.

Notes and references

1 P. G. Wang, T. B. Cai and N. Taniguchi, Nitric Oxide Donors for Pharmaceutical and Biological Applications. Wiley-VCH Verlag GmbH & Co. KGaA, Weinheim, Germany, 2005.

2 P. G. Wang, M. Xian, X. Tang, X. Wu, Z. Wen, T. Cai and A. J. Janczuk, Chem. Rev., 2002, 102, 1091–1134.

3 L. J. Ignarro, Nitric Oxide: Biology and Pathobiology. Elsevier Inc, 2010.

4 L. J. Ignarro, Nitric Oxide Chemistry and Biology, Arch. Pharmacal Res., 2009, 32, 1099–1101.

5 L. Schmetterera and K. Polak, Prog. Retinal Eye Res., 2001, 20, 823–847.

6 H. Jeong, S. Park, K. Park, M. Kim and J. Hong, Mol. Pharmaceutics, 2020, 17, 656–665.

7 J. Aliancy, W. D. Stamer and B. Wirostko, Ophthalmol. Ther., 2017, 6, 221–232.

8 V. Bonfiglio, G. Camillieri, T. Avitabile, G. M. Leggio and F. Drago, Exp. Eye Res., 2006, 83, 1366–1372.

9 J. Cejkova and C. Cejka, Histol. Histopathol., 2015, 30, 893–900.

10 G. S. Park, N. S. Kwon, Y. M. Kim and J. C. Kim, Korean J. Ophthalmol., 2001, 15, 59–66.

11 D. A. Riccio and M. H. Schoenfisch, Chem. Soc. Rev., 2012, 41, 3731–3741.

12 A. B. Seabra and N. Duran, J. Mater. Chem., 2010, 20, 1624–1637.

13 Q. Jia, A. J. Janczuk, T. Cai, M. Xian and Z. P. Wen, Expert Opin. Ther. Pat., 2002, 12, 819–826.

14 S. Sortino, Chem. Soc. Rev., 2010, 39, 2903–2913.

15 P. C. Ford, Nitric Oxide, 2013, 34, 56–65.

16 N. L. Fry and P. K. Mascharak, Acc. Chem. Res., 2011, 44, 289–298.

17 A. Fraix, N. Marino and S. Sortino, Top. Curr. Chem., 2016, 370, 225–257.

18 A. Fraix and S. Sortino, Chem. – Asian J., 2015, 10, 1116–11258.

19 M. Seggio, A. Nostro, G. Ginestra, F. Quaglia and S. Sortino, Int. J. Mol. Sci., 2019, 20, 3735–3743.

20 N. Marino, M. Perez-Lloret, A. R. Blanco, A. Venuta, F. Quaglia and S. Sortino, J. Mater. Chem. B, 2016, 4, 5138–5143.

21 J. Szejtli, Cyclodextrin Technology, Kluwer, Dordrecht, 1998.

22 J. Szejtli, Pure Appl. Chem., 2004, 76, 1825–1845.

23 M. E. Davis and M. E. Brewster, Nat. Rev. Drug Discovery, 2004, 3, 1023–1035.

24 T. Loftsson and D. Douchene, Int. J. Pharm., 2007, 329, 1–11.

25 A. Harada, M. Furue and S. Nozakura, Polym. J., 1981, 13, 777.

26 A. Mazzaglia, M. T. Sciortino, N. Kandoth and S. Sortino, J. Drug Delivery Sci. Technol., 2012, 22, 235–242.

27 S. Monti and S. Sortino, Chem. Soc. Rev., 2002, 31, 287–300.

28 A. Fraix and S. Sortino, Photochem. Photobiol. Sci., 2018, 17, 1709–1727 and references therein.

29 L. Piras, T. A. Theodossiou, M. D. Manouilidou, Y. G. Lazarou, S. Sortino and K. Yannakopoulou, Chem. – Asian J., 2013, 8, 2768–2778.

30 G. Benkovics, M. Perez-Lloret, D. Afonso, A. Darcsi, S. BeÅLni, E. Fenyvesi, M. Malanga and S. Sortino, Int. J. Pharm., 2017, 531, 614–620e.

31 N. Mourtzis, M. Paravatou, I. M. Mavridis, M. L. Roberts and K. Yannakopoulou, Chem. – Eur. J., 2008, 14, 4188–4200.

32 K. Yannakopoulou, L. Jicsinszky, C. Aggelidou, N. Mourtzis, T. M. Robinson, A. Yohannes, E. M. Nestorovich, S. Bezrukov and V. A. Karginov, Antimicrob. Agents Chemother., 2011, 55, 3594–3597.

33 C. Parisi, M. Seggio, A. Fraix and S. Sortino, ChemPhoto- Chem, 2020, 4, 742–748.

34 E. M. Van Buskirk, R. N. Weinreb, D. P. Berry, J. S. Lustgarten, S. M. Podos and M. M. Drake, Am. J. Ophthalmol., 1986, 101(5), 531–534.

35 G. Chidlow, J. Melena and N. N. Osborne, Br. J. Pharmacol., 2000, 130, 759–766. 36 M. Montalti, A. Credi, L. Prodi and M. T. Gandolfi, Handbook of Photochemistry, 3rd edn, CRC Press, Boca Raton, 2006.

37 NBF moiety could fit within the bCD cavity.37a T. Sun, A. Hao, J. Shen and L. Song, Synth. Commun., 2009, 39, 4309–4314.

38 A. Buldt and U. Karst, Anal. Chem., 1999, 71, 3003.

39 C. Sveen, N. Macia, V. Zaremberg and B. Heyne, Photochem. Photobiol., 2015, 91, 272.

40 A. Benesi and J. H. Hildebrand, J. Am. Chem. Soc., 2009, 131(34), 12218–12229.

41 (a) C. Parisi, M. Failla, A. Fraix, B. Rolando, E. Gianquinto, F. Spyrakis, E. Gazzano, C. Riganti, L. Lazzarato, R. Fruttero, A. Gasco and S. Sortino, Chem. – Eur. J., 2019, 25, 11080; (b) C. Parisi, M. Failla, A. Fraix, A. Rescifina, B. Rolando, L. Lazzarato, V. Cardile, A. C. E. Graziano, R. Fruttero, A. Gasco and S. Sortino, Bioorg. Chem., 2019, 85, 18.

Figures and tables

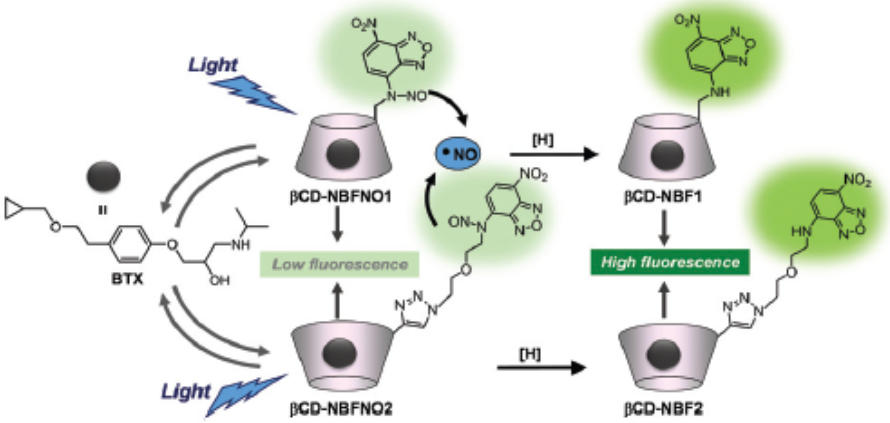

Scheme 1 Structures of **βCD-NBFNO1**, **βCD-NBFNO2**, their respective fluorescent photoproducts **βCD-NBF1**, **βCD-NBF2** formed after NO photorelease, and **BTX** used as guest molecule.

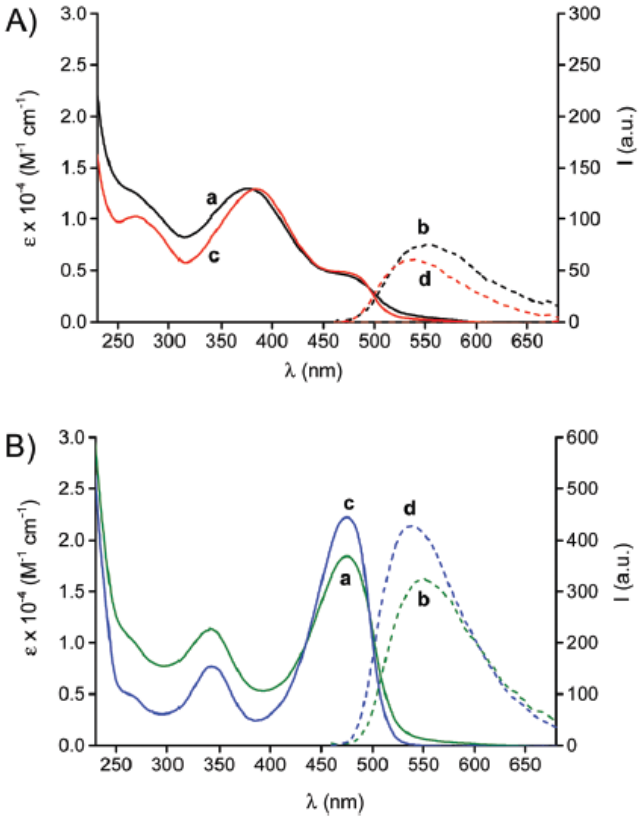

Fig. 1 (A) Absorption and fluorescence emission spectra (λ_{exc} = 450 nm) of aqueous solutions of **βCD-NBFNO1** (a and b) and **βCD-NBFNO2** (c and d). (B) Absorption and fluorescence emission spectra (λ_{exc} = 450 nm) of aqueous solutions of denitrosated **βCD-NBF1** (a and b) and **βCD-NBF2** (a and d). Fluorescence emission spectra were carried out with optically matched solutions of all compounds at the excitation wavelength. T = 25 °C.

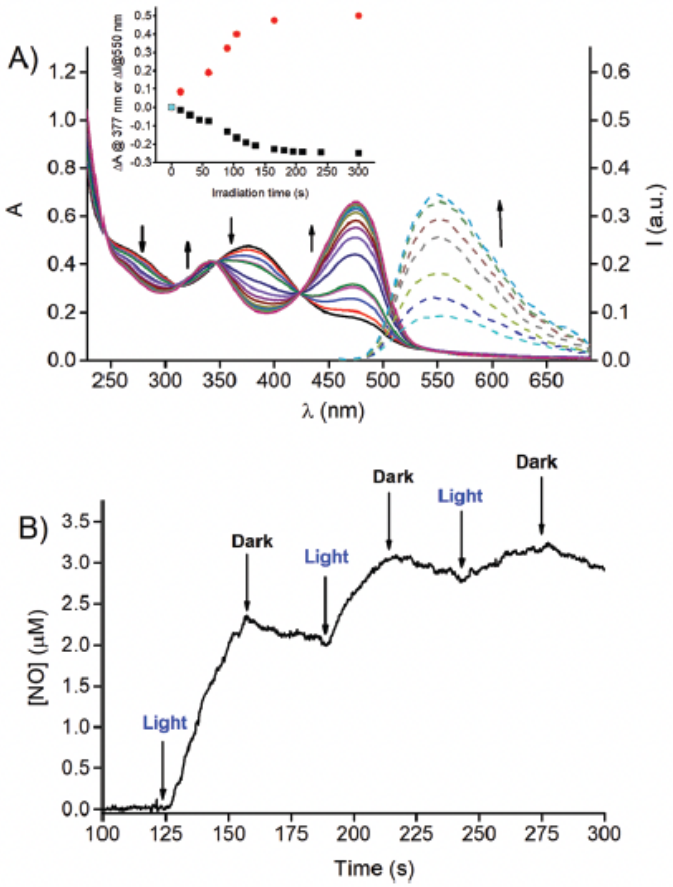

Fig. 2 (A) Absorption (solid lines) and fluorescence emission, (λ_{exc} = 424 nm, isosbestic point) (dotted lines) spectral changes observed upon exposure of an aqueous solution of **βCD-NBFNO1** (35 μM) at λ_{exc} = 405 nm (*ca.* 20 mW cm^{-2}) for time intervals from 0 to 300 s. The arrows indicate the course of the spectral profile with the illumination time. The inset shows the different absorbance changes at λ = 377 nm (■) and fluorescence changes at λ = 550 nm (●), respectively. (B) NO release profile observed for an aqueous solution of **βCD-NBFNO1** (35 μM) upon alternate cycles of irradiation (λ_{exc} = 405 nm, *ca.* 20 mW cm^{-2}) and dark. T = 25 °C.

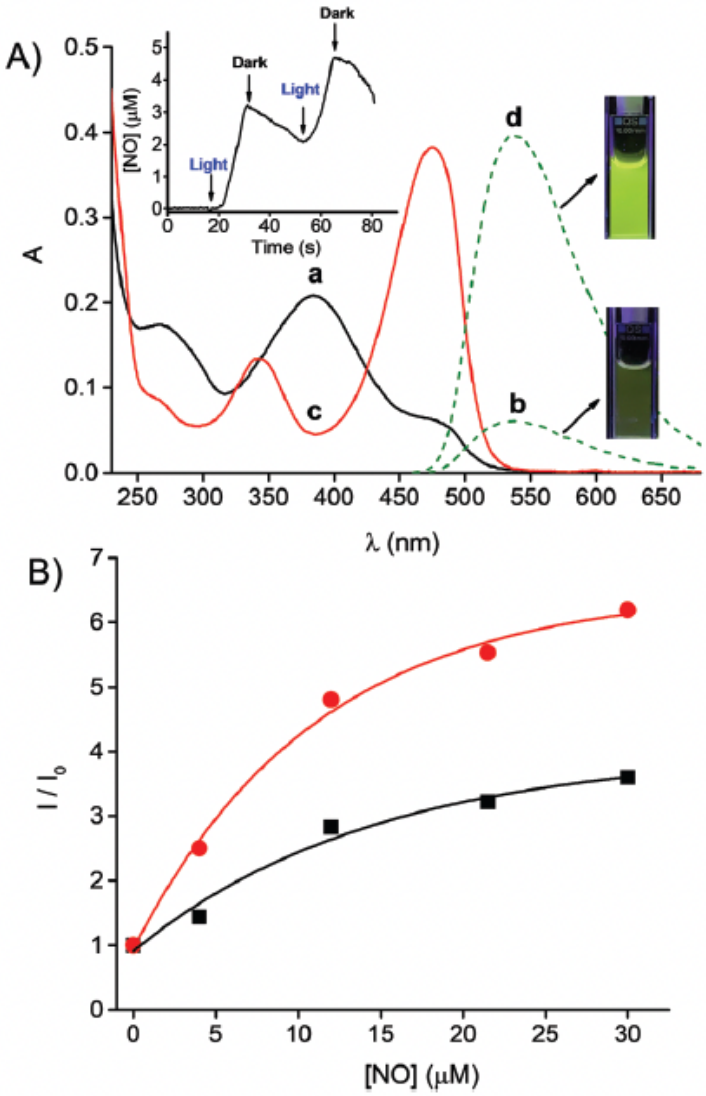

Fig. 3 Fig. 3 (A) Absorption (solid lines) and fluorescence emission, (λ_{exc} = 427 nm, isosbestic point) (dotted lines) spectra changes observed before (a and b) and after the complete photolysis (c and d) at λ_{exc} = 405 nm (*ca.* 20 mW cm^{-2}) of aqueous solution of **βCD-NBFNO2** (16 μM) and actual images of the solutions before (bottom) and after (top) the photolysis acquired upon excitation at λ = 350 nm. The inset shows the NO release profile observed for an aqueous solution of **βCD-NBFNO2** (16 μM) upon alternate cycles of irradiation (λ_{exc} = 405 nm, *ca.* 20 mW cm^{-2}) and dark. (B) Correlation of the fluorescence increase observed upon photolysis of **βCD-NBFNO1** (■) and **βCD-NBFNO2** (●) and the concentration of NO photoreleased. I and I_0 represent the fluorescence intensities at the λ_{max} of emission after and before irradiation, respectively. T = 25 °C.

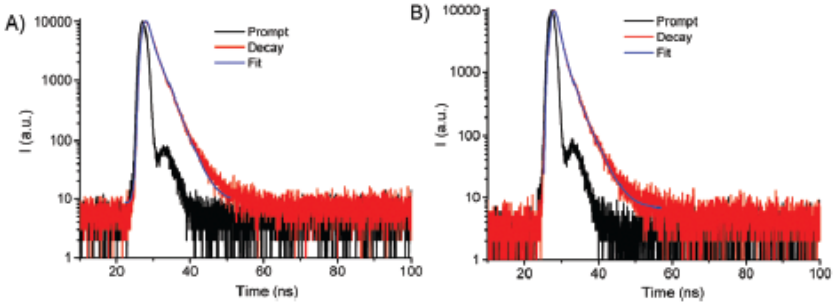

Fig. 4 Fluorescence decay and the related biexponential fitting of the aqueous solution of **βCD-NBFNO1** (40 μM) (A) and **βCD-NBFNO2** (B) recorded at λ_{exc} = 455 nm and λ_{em} = 550 nm.

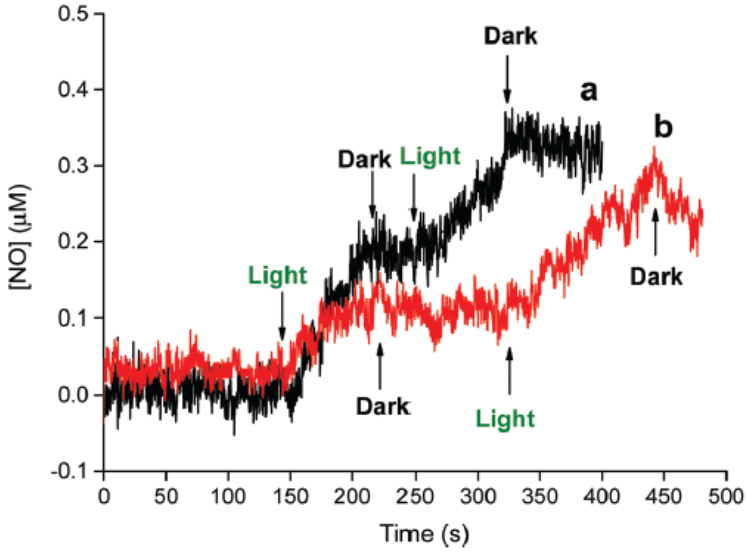

Fig. 5 NO release profiles observed for an aqueous solution of **βCD-NBFNO1** (35 μM, a) and **βCD-NBFNO2** (16 μM, b) upon alternate cycles of irradiation with green light (λ_{exc} = 532 nm, *ca.* 100 mW cm^{-2}) and dark.

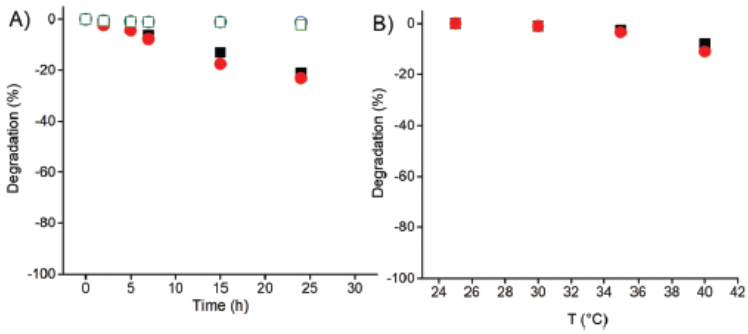

Fig. 6 (A) Dark stability of the aqueous solution of **βCD-NBFNO1** (square) and **βCD-NBFNO2** (circles) incubated in the dark at 25 °C (filled symbols) or 4 °C (open symbols) at different times. (B) Dark stability of the aqueous solution of **βCD-NBFNO1** (square) and **βCD-NBFNO2** (circles) incubated for 15 min at different temperatures.

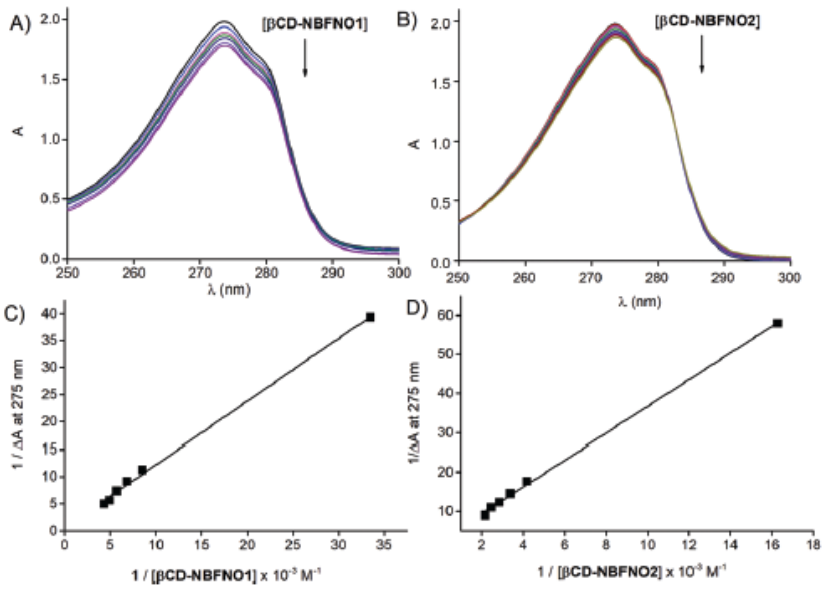

Fig. 7 Absorption spectral changes observed upon addition of different amounts of **βCD-NBFNO1** from 28 μM to 210 μM (A) and **βCD-NBFNO2** from 62 μM to 500 μM (B) to aqueous solutions of **BTX** (1.4 mM). The related double-reciprocal plots and the linear fitting of the data, according to the Benesi–Hildebrand equation, are reported for **βCD-NBFNO1** (C) and **βCD-NBFNO2** (D). T = 25 °C.

Electronic Supplementary Information

Visible Light-Activatable Cyclodextrin-Conjugates for the Efficient Delivery of Nitric Oxide with Fluorescent Reporter and their Inclusion Complexes with Betaxolol

Mimimorena Seggio,[a] Sara Payamifar,[a,b,§] Aurore Fraix,[a] Eszter Kalydi,[c,d] Petr Kasal,[e] Ovidio Catanzano,[f] Claudia Conte,[g] Fabiana Quaglia[g,*] and Salvatore Sortino[a,*]

[a] *PhotoChemLab, Department of Drug and Health Sciences, University of Catania, Catania, Italy. Email: ssortino@unict.it*
[b] *Organic Chemistry Institute for Advanced Studies in Basic Sciences (IASBS), Zanjan, Iran.*
[c] *CycloLab Ltd., H-1097 Budapest, Illatos út 7, Hungary.*
[d] *Department of Pharmacognosy, Semmelweis University, Budapest, H-1085 Üllői út 26, Hungary.*
[e] *Department of Organic Chemistry, Charles University in Prague, Hlavova 2030/8 128 43 Prague 2 Czech Republic.*
[f] *Institute for Polymers, Composites and Biomaterials, CNR, Via Campi Flegrei 34, 80078 Pozzuoli, Napoli, Italy.*
[g] *Drug Delivery Laboratory, Department of Pharmacy, University of Napoli Federico II, Via Domenico Montesano 49, 80131, Napoli, Italy. Email: quaglia@unict.it*
[§] *S. P. carried out the work at the University of Catania during her stage from the IASBS.*

Synthetic Description

In Fig. S1, the synthesis scheme for βCD-NBFNO1 is shown. 6-Monodeoxy-6-monoamino free base (2) was obtained by precipitation of the corresponding hydrochloride salt with concentrated ammonia. The nitrobenzofurazanyl group was installed onto the CD scaffold without using any additional base in order to avoid the formation of NBF-related by-products; it is worth noticing that 4-chloro-7-nitrobenzofurazan would react with any additional base in the mixture thus creating new chromophoric species and complicating the purification process. The βCD-NBF1 derivative was isolated by chromatography. βCD-NBFNO1 was obtained by reacting βCD-NBF1, solubilized in a mixture of DMSO/CH_3COOH 1:1 with $NaNO_2$. The solution was stirred at 0 °C for 1 hour and at room temperature for 2 days. The reaction mixture was precipitated with acetone. The solid was filtered-off, and a dark yellow powder was obtained.

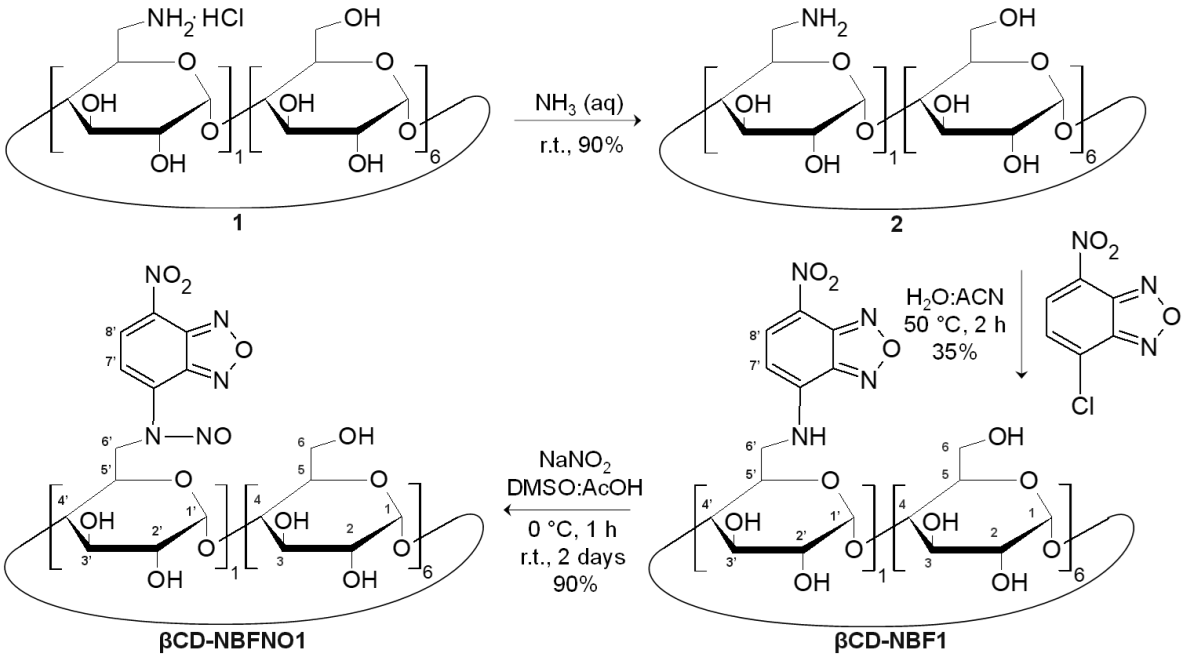

Figure S1: Synthesis scheme for βCD-NBFNO1.

In Fig. S2, the synthesis scheme for βCD-NBFNO2 is shown. Regioselective 2-*O*-monopropargylation of βCD (3) was achieved in DMSO with LiH and propargyl-bromide as previously reported.[1S] The conjugation of 2-*O*-monopropargyl-βCD (4) and azido-diethylene glycol-nitrobenzofuraran linker (5) was based on a copper-assisted azide–alkyne cycloaddition. The click reaction was performed in DMF mixture at 60 °C with copper(I) bromide as catalyst. The reaction crude was purified by preparative direct-phase chromatography on silica gel yielding βCD-NBF2 in good purity. βCD-NBFNO2 was obtained by reacting βCD-NBF2, solubilized in a mixture of DMSO/CH_3COOH 1:1 with $NaNO_2$. The solution was stirred at 0 °C for 1 hour and at room temperature for 2 days. The reaction mixture was precipitated with acetone. The solid was filtered-off, and a dark yellow powder was obtained.

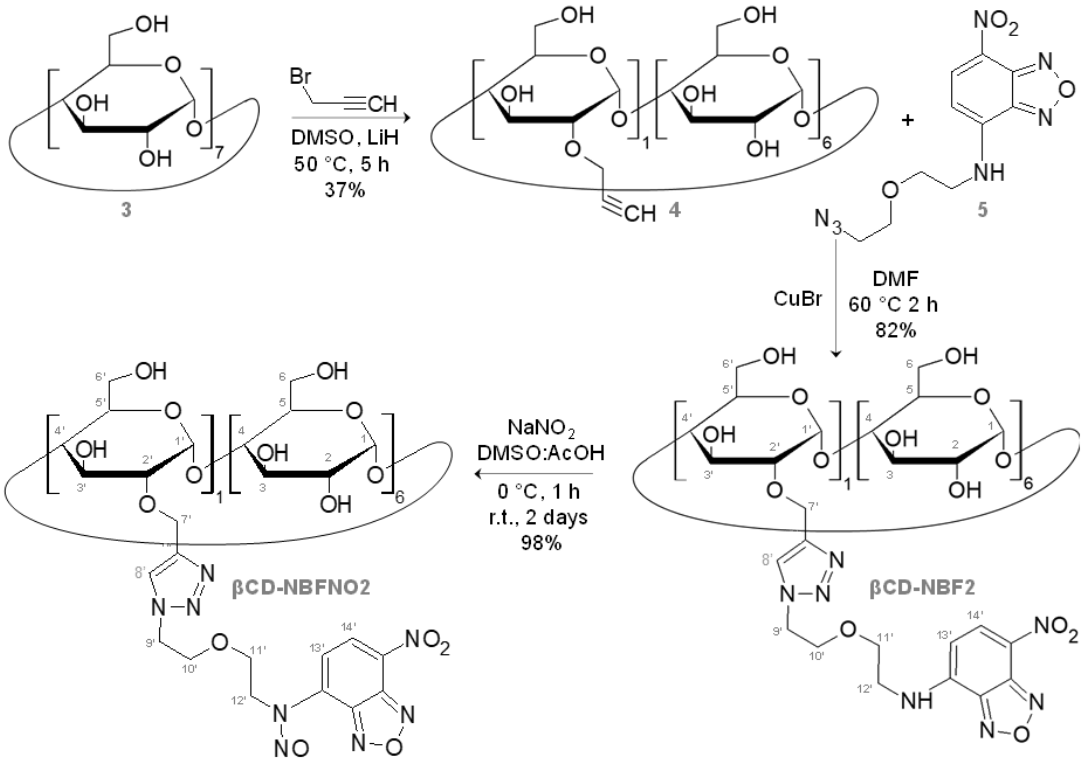

Figure S2: Synthesis scheme for βCD-NBFNO2.

The synthetic strategy for compound 5 is shown in Fig. S3. The preparation of the linker was divided in two parts. First 2-(2-azidoethoxy)ethan-1-amine (L4) was synthesized by modifications of existing synthetic procedures.[2S,3S] Compound 5 was prepared globally in 4 synthetic steps starting from the commercially available diethylene glycol (L1). The diol was exhaustively tosylated in DCM with potassium hydroxide (biphasic system) and the product, diethylene glycol di(*p*-toluenesulfonate) (L2), was effectively isolated by liquid-liquid extraction. Compound L2 was converted to the corresponding diazido diethylene glycol (L3) in DMF with excess of sodium azide. Isolation of the compound L3 was based on liquid-liquid extraction. Partially reduction of diazido diethylene glycol based on Staudinger reaction and *ad-hoc* developed work-up afforded the 2-(2-azidoethoxy)ethan-1-amine (L4) in good yield and purity. Chromophore 4-chloro-7-nitrobenzofurazan was finally reacted with compound L4 in absolute ethanol. Compound 5 was isolated by liquid-liquid extraction and purified by direct-phase chromatography on silica gel with DCM as eluent in isocratic elution.

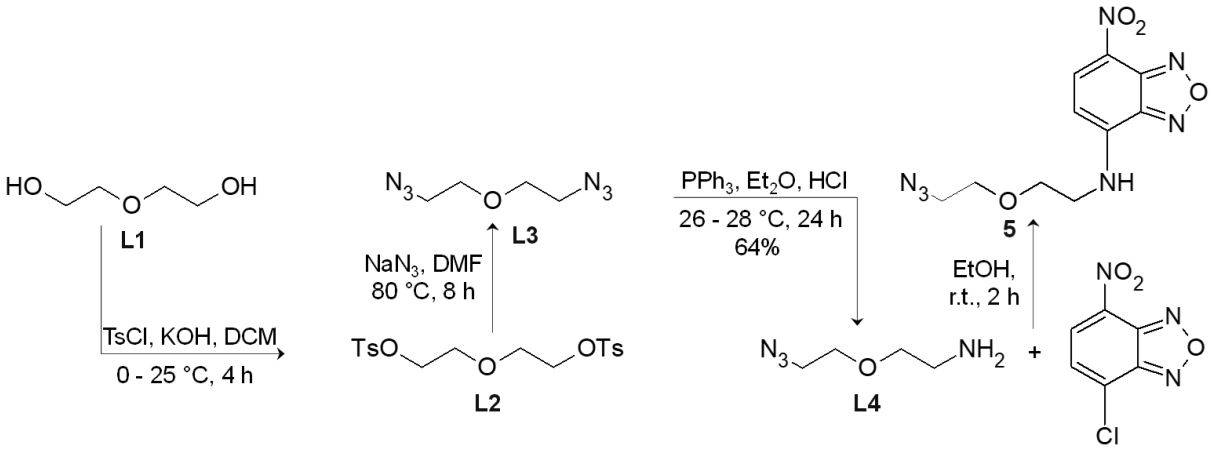

Figure S3: Synthesis scheme for compound 5.

6-Monodeoxy-6-monoamino-βCD free base (2)

6-Monodeoxy-6-monoamino-βCD hydrochloride (11.70 g, 10 mmol) was solubilized in water (50 mL) and the solution was added to ammonia 25% solution (80 mL) under vigorous stirring. The white precipitate was filtered on a sintered glass filter (porosity 3), the solid was washed with methanol (2 x 15 mL) and placed into a vacuum drying box overnight in the presence of P_2O_5 and KOH (~10 g, 88% yield).

m.p.: 203-205 °C (dec.). R_f: 0.26-0.29 in 1,4-dioxane:25% aqueous NH_3:1-propanol=10:7:3.

^{1}H-NMR (D_2O): δ(ppm) 5.10-5.05 (m, 7H, H1, H1'), 4.10-4.05 (m, 1H, H3'), 3.99-3.75 (bs, 25H, H3, H5, H6), 3.67-3.47 (bs, 15H, H2, H4, H6'), 3.26-3.20 (m, 1H, H6').

^{13}C-NMR (125 MHz, D_2O): δ(ppm) 101.94 (C1), 101.38 (C1'), 83.02 (C4'), 81.36 (C4), 81.30 (C4), 81.27 (C4), 81.24 (C4), 73.23 (C3), 73.00, 72.59, 72.17, 71.94, 68.00 (C3'), 60.45 (C6), 40.36 (C6').

βCD-NBF1

4-chloro-7-nitrobenzofurazan (NBF-Cl) (0.2 g, 1 mmol) dissolved in acetonitrile (5 mL) was added to an aqueous (50 mL) solution of (2) (1.13 g, 1 mmol) and the reaction mixture was heated at 50 °C for 2 h. The solvents were completely evaporated under reduced pressure (T=60 °C), the crude was dissolved in water (20 mL) and extracted with dichloromethane (2 x 20 mL). The aqueous phase was suspended with silica gel (5 g) and the mixture was evaporated under reduced pressure until dryness. This crude mixture thus preabsorbed onto silica was purified by chromatography over silica with CH_3OH:H_2O:HCOOH (0.05%) 9:1:0.5 as eluent in isocratic elution. The fractions were analyzed by TLC and those containing βCD-NBF1 were combined and concentrated under reduced pressure. The viscous solution was neutralized (NaOH 0.1 N) and precipitated with MeOH (50 mL). The obtained solid was filtered on a sintered glass filter (porosity 3), washed with methanol (2 x 15 mL) and placed into a vacuum drying box overnight in the presence of P_2O_5 and KOH (dark brown solid, 0.45 g, 35% yield).

R_f: 0.56, (9:1 MeOH:H_2O); ^{1}H-NMR (500 MHz DMSO-d_6): δ(ppm) 8.35 (m, 1H, H8'), 6.20 (bs, 1H, H7'), 5.11-4.94 (m, 7H, H1), 3.35-4.26 (bs, 42H, H2, H3, H4, H5, H6).

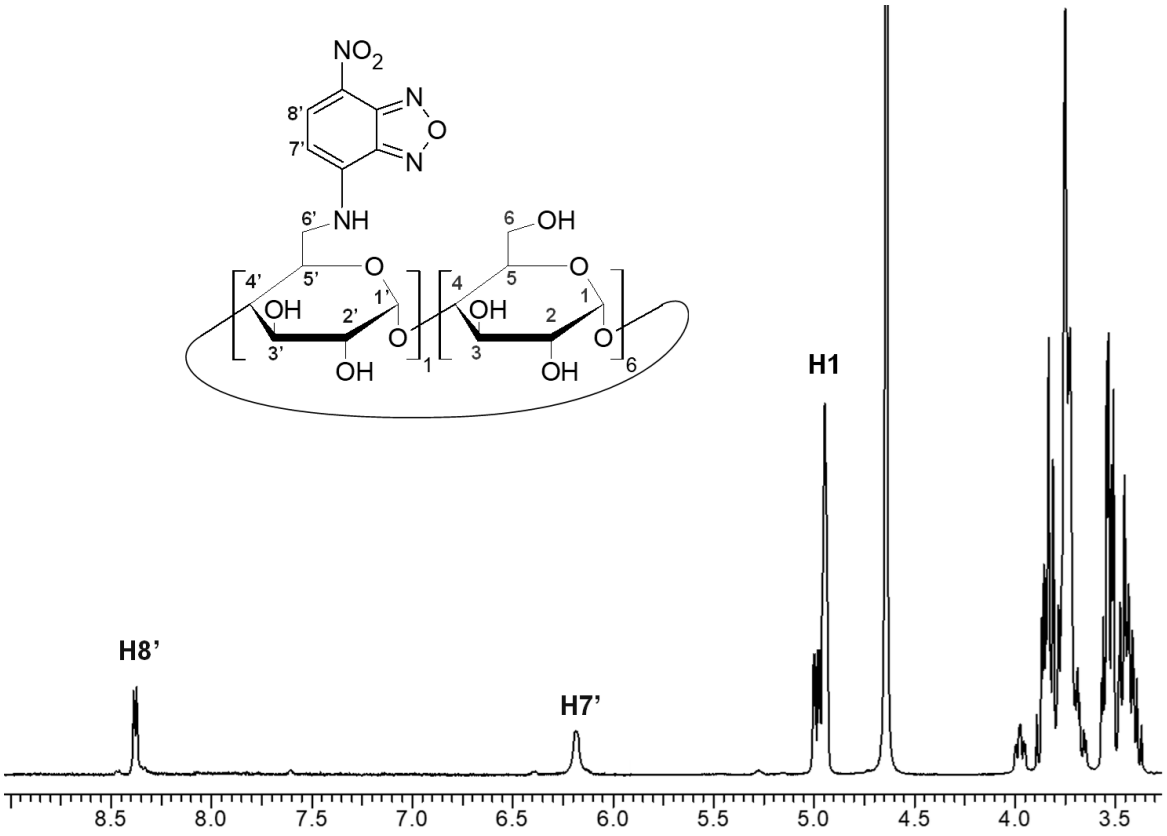

^{1}H NMR spectrum of βCD-NBF1 with partial assignment (500 MHz, DMSO, 298.15 K).

βCD-NBFNO1

βCD-NBF1 (50 mg, 0.04 mmol) was solubilized in a mixture of DMSO/CH_3COOH 1:1 (2 mL). After complete solubilization, the solution was cooled at 0 °C with an ice bath and $NaNO_2$ (100 mg, 1,45 mmol) was added; the solution was stirred at 0 °C for 1 hour and at room temperature for 2 days. The reaction mixture was precipitated with acetone (40 mL). The solid was filtered-off on a glass filter (porosity 3), extensively washed with acetone (2 x 10 mL) and dried until constant weight in a vacuum drying box (51 mg; 98% yield) and a dark yellow powder was obtained.

R_f = 0.70 (9:1 MeOH:H_2O);^{1}H-NMR (500 MHz DMSO-d_6): δ(ppm) 8.9 (d, 1H, H8'), 7.83 (d, 1H, H7'), 5.11-4.8 (m, 7H, H1), 2.9-3.95 (bs, 42H, H2, H3, H4, H5, H6).

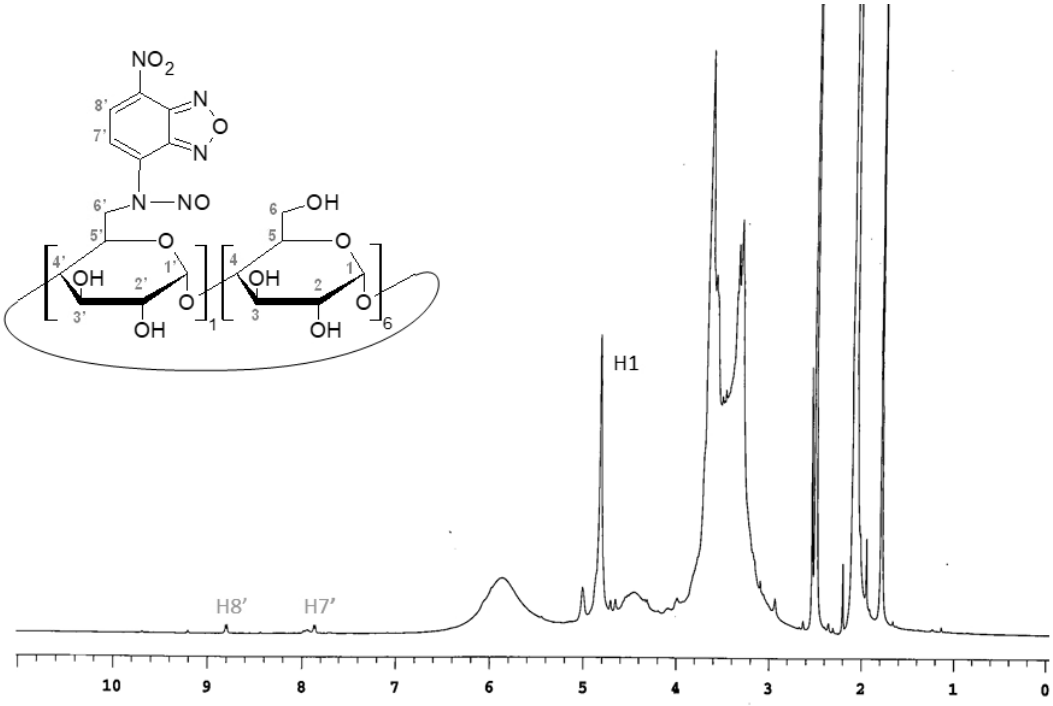

^{1}H-NMR spectrum of βCD-NBFNO1 with partial assignment (DMSO-d_6, 500 MHz, 298.15 K).

2-O-Monopropargyl-βCD (4)

Lithium hydride (53 mg, 6.608 mmol) was added to βCD solution 1 (5 g, 4.405 mmol) in dry DMSO (75 mL). The resulting suspension was stirred under N_2 at room temperature until it became clear (12-24 h). Propargyl bromide (solution in toluene, 80% w/w, 491 μL, 4.405 mmol) and a catalytic amount of lithium iodide (~5 mg) were then added and the mixture was stirred at 50 °C in the absence of light for 5 h. TLC (10:5:2 CH_3CN:H_2O:25% aqueous NH_3) showed four spots with R_f values of 0.75, 0.65, 0.50, and 0.30, the last two corresponding to monopropargylated and nonpropargylated βCD, respectively. The solution was poured into acetone (800 mL), the precipitate was filtered on a sintered glass filter (porosity 4) and washed thoroughly with acetone. The resulting solid was transferred into a round-bottom flask and dissolved in a minimum volume of water. Silica gel (10 g) was added and the solvent was removed under vacuum until powdered residue was obtained. This crude mixture was applied on top of a column of silica (25 x 6 cm), and chromatography (10:5:2 CH_3CN:H_2O:25% aqueous NH_3) yielded, after freeze-drying, 2-*O*-monopropargyl-βCD (***4***) (1.912 g, 1.63 mmol, 37%) as white solid.

The material decomposes at 239-245 °C; [α]25D +126 (c 0.25, H_2O); R_f = 0.50 (10:5:2 CH_3CN–H_2O–25% aqueous NH_3); IR (KBr): 3397, 2923, 2117, 1646, 1156, 1081, 1029 cm^{-1}; ^{1}H NMR (500 MHz, DMSO-d_6) δ(ppm) 5.98 (br d, 1H, OH), 5.88 (br s, 1H, OH), 5.79-5.69 (m, 10H, OH), 4.98 (d, 1H, 3J = 3.6 Hz, H1'), 4.84-4.82 (br s, 6H, H1), 4.54 (t, 1H, J = 5.6 Hz, OH), 4.50-4.45 (m, 8H, OH, CHC≡), 4.38 (dd, 1H, 2J = 15.8 Hz, 4J = 2.4 Hz, CHC≡), 3.78 (t, 1H, 3J = 9.8 Hz, H3'), 3.64-3.53 (m, 27H; H3, H5, H6a, H6b), 3.51 (t, 1H, 4J = 2.4 Hz, ≡CH), 3.43-3.40 (m, 2H, H2',H4'), 3.36-3.29 ppm (m, 12H, H2, H4); ^{13}C NMR (125 MHz, DMSO-d_6) δ 102.0-101.7 (C1), 100.1 (C1'), 82.2-81.4 (C4), 79.9 (C≡), 79.1 (C-2'), 77.8 (≡CH), 73.3-

71.7 (C2, C3, C), 72.6 (C3'), 60.1-59.7 (C6), 58.8 ppm ($CH_2C\equiv$); MALDI-TOF: [M+Na]+ calcd for $C_{45}H_{72}O_{35}Na$, 1195.4; found: 1195.58.

Compound 5

Diethylene glycol (L1) (50.0 g, 0.47 mol) was dissolved in CH_2Cl_2 (480 mL) and TsCl (180.0 g, 0.942 mol) was added. The solution was cooled to 0 °C and crushed KOH (211.0 g, 3.77 mol) was slowly added. The suspension was additionally stirred at 0 °C for 3 h. The reaction mixture was monitored by TLC using hexane:EtOAc 1:1 as eluent and detection was achieved with potassium permanganate solution. The mixture was warmed to room temperature and $CHCl_3$ (400 mL) was added. The mixture was extracted with water (3 x 400 mL) and the organic phase was dried with $MgSO_4$ (25 g). The desiccant was filtered off and the filtrate was evaporated on a rotary evaporator at 40 °C. The product was dried at room temperature using an oil rotary pump. Diethylene glycol ditosylate (L2) (169.6 g, 0.41 mol) was dissolved in DMF (800 mL) and NaN_3 (106.7 g, 1.64 mol) was added. The suspension was stirred at 80 °C for 8 h. The reaction mixture was monitored by TLC using hexane:EtOAc 1:1 mixture as eluent and detection was achieved with potassium permanganate solution. The suspension was cooled to room temperature and water (750 mL) was added. The solution was extracted with Et_2O (1600 mL). The organic phase was then extracted with water (3 x 1600 mL). It was verified by ^{1}H NMR that the mixture was free of DMF residues. The organic phase was then concentrated to a volume of approximately 800 mL on a rotary evaporator at room temperature To the solution was added 1 M HCl (800 mL), and the biphasic mixture was stirred vigorously. PPh_3 (123.0 g, 0.47 mol) was then added in small portions and the mixture was stirred overnight. The reaction mixture was monitored by TLC using hexane:EtOAc 1:1 mixture for the starting diazide (L3) and CH_2Cl_2:MeOH:25% aqueous NH_3 3:3:1 mixture for the product (L4); detection was achieved with potassium permanganate. The precipitated triphenylphosphine oxide was filtered off and washed with water. The organic phase was separated and the aqueous solution was subsequently extracted with Et_2O (3 x 500 mL). The aqueous solution was cooled to 0 °C and KOH (300 g) was slowly added. The basic aqueous solution was then extracted with CH_2Cl_2 (6 x 600 mL). The organic phase was then dried with $MgSO_4$ (18 g), the desiccant was filtered off and the filtrate was evaporated at 30 °C on a rotary evaporator. The product was dried at room temperature using an oil rotary pump. The product was obtained as an yellowish oil, in 64% yield (39 g). IR(KBr): 3357, 2860, 2101 ν(azide), 1595, 1440, 1344, 1269, 1120 cm^{-1}. ^{1}H NMR (300 MHz, $CDCl_3$):δ = 3.65 (t, *J* = 5.2 Hz, 2H, H-3), 3.52 (t, *J* = 5.1 Hz, 2H, H-2), 3.39 (t, *J* = 5.1 Hz, 2H, H-4), 2.88 (t, *J* = 5.1 Hz, 2H, H-1) ppm. ^{13}C NMR (100 MHz, $CDCl_3$):δ = 73.15 (C-2), 70.00 (C-3), 50.80 (C-4), 41.73 (C-1) ppm. ESI MS: for $C_4H_{10}N_4O$calcd: *m/z* 130.1, found 131.2 $[M+H]^+$. HRMS: for $C_4H_{10}N_4O$calcd: *m/z* 130.0855, found 131.0933 $[M+H]^+$, Δ 4.6 ppm. ^{1}H NMR spectrum was consistent with the literature (Klein et al.). NBF-Cl (0.8 g, 4 mmol) was solubilized in EtOH (20 mL) and slowly added to a EtOH solution (10 mL) of 2-(2-azidoethoxy)ethan-1-amine (L4) (1.3 g, 10 mmol) under vigorous stirring. The mixture was stirred at r.t. for 2 h. The reaction was monitored by TLC (DCM:hexane 8:2) and detection was achieved under UV-Lamp at 254 nm. The reaction mixture was evaporated under reduced pressure at 40 °C and the obtained oil was diluted with DCM (50 mL) and extracted with water (3 x 50 mL). The organic phase was extracted with

HCl 1 M (3 x 100 mL), dried over $MgSO_4$ and concentrated under reduced pressure. The obatined oil was purified by chromatography with DCM as eleunt in isocratic elution. the product was concentrated under reduced pressure and a dark oil was obtained (1.2 g, 42% yield).

R_f = 0.20 (8:2 DCM:Hexa$_n$e); ^{1}H NMR (500 MHz, $CDCl_3$) δ(ppm) 8.47 (d, 1H, H2), 6.72 (br s, 1H, NH), 6.23 (d, 1H, H3), 3.88 (t, 2H, H8), 3.76-3.74 (m, 4H, H7-H9), 3.45 (t, 2H, H10).

βCD-NBF2

Compound 5 (0.1 g, 0.35 mmol) was solubilized in DMF (5 mL) and added to a DMF solution (20 mL) of 2-*O*-monopropargyl-βCD (0.36 g, 0.31 mmol). CuBr (12 mg, 0.083 mmol) was added to the solution under vigorous stirring and the reaction mixture was heated at 60 °C for 2 h. The progress of the reaction was monitored by TLC (10:2.5:1 ACN:H_2O:25% aqueous NH_3). The crude reaction was filtered on a celite pad to remove copper-related material and the pad was extensively washed with DMF (3 x 10 mL). The filtrate was suspended with silica gel (5 g) and the solvent was removed under vacuum until a powdered residue was obtained. This crude mixture thus preabsorbed onto silica was purified by chromatography over silica with 10:2.5:1 ACN:H_2O:25% aqueous NH_3 as eluent in isocratic elution. The fractions were analyzed by TLC and those containing βCD-NBF2 were combined and concentrated under reduced pressure until dryness. The solid was solubilized in H_2O (5 mL) and dialyzed for 48 h against deionized water. The dialysate was finally concentrated until dryness under reduced pressure. The brown solid was placed into a vacuum drying box overnight in the presence of P_2O_5 and KOH (0.37 g, 82% yield).

R_f = 0.66 (9:1 MeOH:H_2O); ^{1}H NMR (500 MHz, DMSO-d_6) δ(ppm) 8.29 (d, 1H, H14'), 7.89 (s, 1H, H8'), 6.09 (br s, 1H, H13'), 4.94-4.69 (m, 7H, H1), 4.61 (overlapping with HDO signal, br s, 2H, H7'), 4.46 (m, 2H, H9'), 3.92-3.20 (m, 48H, H2, H3, H4, H5, H6, H10', H11', H12'); ^{13}C NMR (125 MHz, DMSO-d_6) assignment based on DEPT-edited HSQC spectrum δ 138.64 (C14'), 126.16 (C8'), 102.55-101.08 (C1), 81.79-80.27 (C4, C2), 74.09 (C5), 72.58 (C2), 72.57 (C10'), 72.18 (C3), 69.54 (C12'), 68.73 (C11'), 65.11 (C7'), 60.66 (C6), 51.22 (C9').

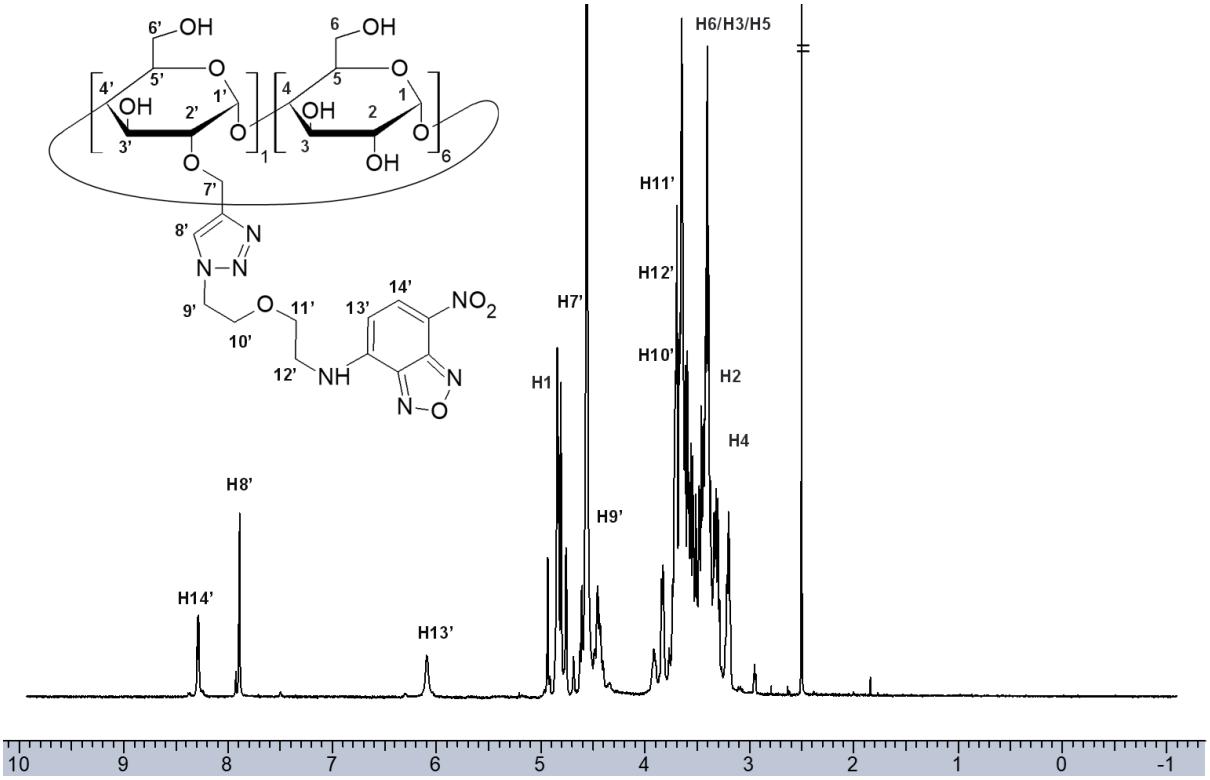

^{1}H-NMR spectrum of βCD-NBF2 with assignment (DMSO-d_6, 600 MHz, 298.15 K).

βCD-NBFNO2

βCD-NBF2 (56 mg, 0.04 mmol) was solubilized in a solution of DMSO/CH_3COOH 1:1 (2 mL). After complete solubilization, the solution was cooled at 0 °C with an ice bath and $NaNO_2$ (100 mg, 1,45 mmol) was added;. the solution was stirred at 0 °C for 1 hour and at room temperature for 2 days. The reaction mixture was precipitated with acetone (40 mL). The solid was filtered-off on a glass filter (porosity 3), extensively washed with acetone (2 x 10 mL) and dried until constant weight in a vacuum drying box (51 mg; 98% yield) and a dark yellow powder was obtained.

R_f = 0.85 (9:1 MeOH:H_2O); ^{1}H NMR (600 MHz, DMSO-d_6) δ (ppm) 8.8 (d, 1H, H14'), 8.03 (br s, 1H, H13'), 7.71 (s, 1H, H8'), 4.97-4.45 (m, 7H, H1), 4.51 (br s, 2H, H7'), 4.4 (m, 2H, H9'), 4.2-2.80 (m, 48H, H2, H3, H4, H5, H6, H10', H11', H12');

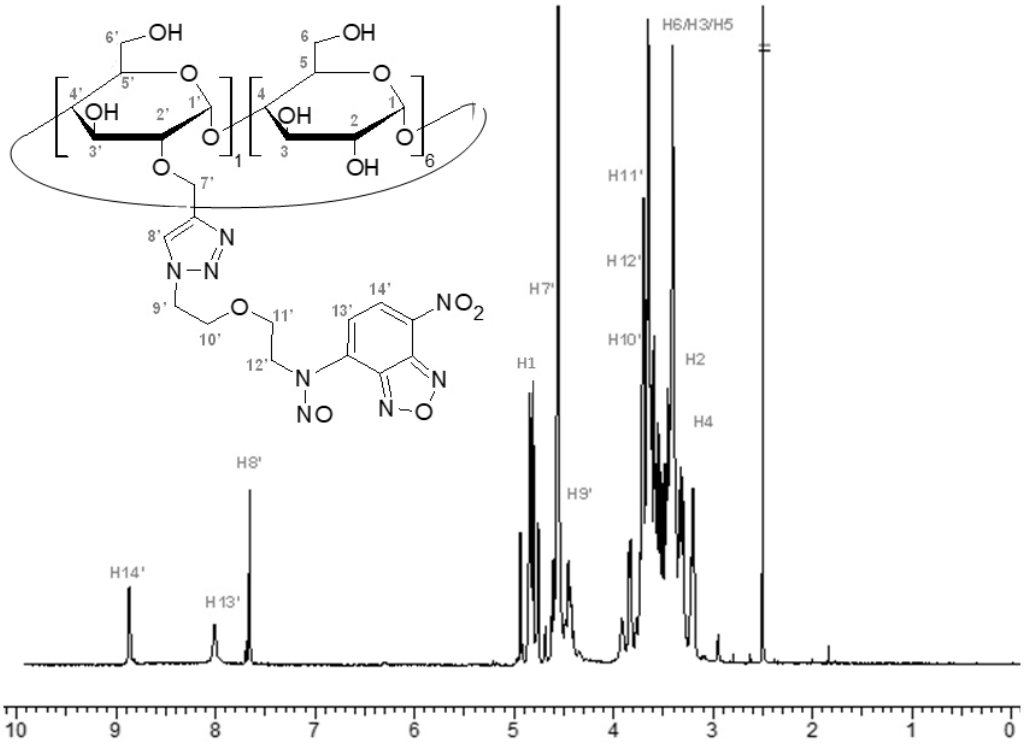

^{1}H-NMR spectrum of βCD-NBFNO2 with assignment (DMSO-d_6, 600 MHz, 298.15 K).

1S. Synthesis of 2I-*O*-propargylcyclomaltoheptaose and its peracetylated and hepta(6-*O*-silylated) derivatives, **2020**, In book: Carbohydrate Chemistry: Proven Synthetic Methods, Volume 5 (forthcoming) Publisher: CRC Press, Taylor & Francis Group.

2S. Bonger, K.M., van den Berg, R.J.B.H.N., Heitman, L.H., IJzerman, A.P., Oosterom, J., Timmers, C.M., Overkleeft, H.S., and van der Marel, G.A. 2007 Jul 15;15(14):4841-56.

3S Klein, E., DeBonis, S., Thiede, B., Skoufias, D.A., Kozielski, F., and Lebeau, L. (2007). New chemical tools for investigating human mitotic kinesin Eg5. Bioorg. Med. Chem. 15, 6474–6488